DROP IMPACT ON POROUS MEDIA

A.N. Lembach, I.V. Roisman and C. Tropea

Center of Smart Interfaces
Institute of Fluid Mechanics and Aerodynamics
Technische Universität Darmstadt, Petersenstr. 32, 64287 Darmstadt, Germany
lembach@csi.tu-darmstadt.de, +49 6151 16 6606

ABSTRACT
This experimental study describes a drop of liquid impacting onto a porous substrate. The interest is on the drop behavior above the surface and especially underneath. There are several applications where this phenomenon plays a major role, like ink jet printing or spray coating. There are already several studies available [1-13], looking at the final state of an absorbed droplet, or simulating the process numerical. For the first time it is now possible to observe the liquid motion above and underneath simultaneously. The liquid has the same refraction index as the porous medium. This, and a small porous depth in the light path gives a clear image of the filled volume inside. This parametric study is comparing the penetration with the Washburn equation[14] and is describing general tendencies. It is shown that different wetting regimes exist and influence the penetration.

INTRODUCTION

Ink jet printing, penetration of rain into walls of a building, needle less injection, coating of porous materials, irrigation of fields, these are all examples for applications which include a drop impacting on a porous media. In Fig. 1 a sketch of the general outcome is shown. The drop spreads on impact, resulting in a thin film with a thick rim, just like an impact on a flat impermeable substrate. If the impact velocity reaches a critical limit, several droplets will emerge through splash [15]. Depending on the porous medium the drop will penetrate fast or slow. This study gives some new insight into this process. Until now only Magnetic Resonance Imaging or X-ray were possible options to see inside the porous medium, but these are either too slow or don't provide enough resolution to observe an impacting drop. A new method is presented in the study at hand. In Fig. 2 a typical series of images obtained in this study is shown.

The Washburn equation [14] is probably the first description of a liquid drop penetrating the substrate without any impact beforehand.

$$L^2 = \frac{\sigma \cdot D_{Pore} \cdot t}{4 \cdot \mu} \qquad (1)$$

Where L is the penetration length, σ the surface tension, D_{Pore} the pore diameter, t the time and μ the dynamic viscosity.

POROUS TARGETS

The porous targets used in this study are made from microscope slides and glass beads. A slit of 1.2 mm is formed with the microscope slides and filled with the glass beads. The slides are glued with 'Thermokitt' a ceramic two component glue, which can withstand high temperatures. The glass beads are filtered to obtain only spherical beads and a small range of diameters. Inside the slit the beads are shaken with an ultrasonic vibrator in order to obtain almost perfect packing. This procedure results in a porosity of ϕ = 0.36. Since only spheres are used for the target production, the porosity is the same for the different sizes. To prevent any movement of the beads during the experiments the targets are sintered. Due to the liquid-glass-transition it is not easy to maintain the right combination of temperature-time curve. With constant 735 °C for one to two hours and a cool down for several hours, it is achieved to connect the beads just at the contact points, while keeping them almost perfectly spherical. Most critical is the cool-down. If done too fast, the immediate result is cracking of the microscope slides. Due to the short sintering the microscope slides will not melt together, but will bend if not supported. The exact time and temperature values depend on the oven used and on the target and glass bead size. In Fig. 3 a typical target is shown.

EXPERIMENTAL PROCEDURE

A sketch of the experimental setup can be seen in Fig. 4. Drops are released from a syringe in different heights resulting in different impact velocities. The impact on the porous targets is illuminated with a LED light source. The light is parallelized with a lens, resulting in a perfectly white

background for shadowgraphy. On the other side of the target, the process is captured by a high speed camera at about 10kfps. This way the impact process is captured above and underneath the surface at the same time. Only the perfect brightness setting can be different for above and underneath, since the porous media refracts some light.

It is possible to observe a drop impact of purified water, but the images are far from perfect. Examples can be seen in Fig. 5. Much better results are obtained by using a mixture of Toluene and Diiodomethan. With this mixture it is possible to perfectly match the refraction index. The impacting droplet is bigger than the porous slit. This results in a complete filling of the porous medium between the microscope slides. The areas filled by the liquid stop refracting the light at the glass beads. This results in a perfect transparency of this area. As shown in Fig. 2, this area is seen completely white, showing a sharp edge for the advancing liquid front. In this parametric study, the liquid, the drop size, the impact velocity, the pore size and the wettability are varied. The hydrophobic and hydrophilic characteristics are achieved with dip coatings from Company Evonik: 'Tego Top 210' and 'No drop'. The Toluene mix removes these coatings, that is why still a lot of measurements with water are used, even if the image processing is more difficult. An overview of the parameters is shown in table1. For the water the typical properties are measured: surface tension σ = 73 mN/m; viscosity μ = 0.96 mPas; contact angle(glass) Θ = 20°±5°; The Toluene- Diiodomethan mix is also measured: surface tension σ = 23 mN/m; viscosity μ = 0.66 mPas; contact angle(glass) Θ = 3°±1°;

IMAGE PROCESSING

The images obtained by the high speed camera are analyzed in the next step by a routine written in Matlab. In Fig. 5 two results of the automatic detection of the liquid front inside the porous media are shown. The penetration width and depth is measured.

RESULTS AND DISCUSSION

In Fig. 6 a typical measurement is shown. The penetration width is higher than the penetration depth in most cases. Three phases can be observed for the penetration, they are separated by the vertical lines. The first phase is simultaneous with the first spreading above the surface and shows a quick penetration. The second phase still shows penetration, but at a much lower penetration rate. In this phase the drop on the surface is performing some oscillations. The oscillations above can also excite oscillations underneath. The drop inertia of the impact movement is all transformed or dissipated already. Only the Laplace pressure [16] can be still considered as driving from above the surface.

$$\Delta p = \sigma \cdot \left(\frac{1}{R_1} \cdot \frac{1}{R_2} \right) \qquad (2)$$

In the third phase the drop is completely penetrated into the substrate and the penetration comes to a halt. Only at these small time intervals this seems to be a real halt. On a longer time axes it can be seen that the decrease due to evaporation starts immediately. The first phase results in less penetration depth than width, but the second phase is longer for the depth, resulting in a caching up. The slope for the different phases is measured, as it is the penetration rate, or penetration velocity. In Fig. 6 the Washburn curve is shown for comparison. The first phase is often in the range of the measured values, but from the second phase on, the difference becomes only bigger. This is, of course because the Washburn curve does not account for a limited drop on the substrate. The predicted penetration is even faster than the measured. Since the impact pressure should help the penetration compared to the still drop in the Washburn case, the measured value is expected to be higher than the Washburn curve.

A big difference to most measurements is observed with the 'No drop' coating, which is highly wettable for water. One example is shown in Fig. 7. It can be clearly seen that the second phase of slow penetration is much longer and also resulting in much higher values. The initial drop radius r = 1.04 mm results in a Liquid Volume of:

$$V = \frac{4}{3} \cdot r^3 \cdot \pi = 4.7\text{mm}^3 \qquad (3)$$

With the penetration ½ width of 8mm at 70sec, the volume would, at complete filling, allow a depth of:

$$a = \frac{V \cdot 2}{\pi \cdot b \cdot b_{slit} \cdot \phi} = 0.8\text{mm} \qquad (4)$$

Assuming the penetrating liquid front has the shape of an ellipse with b = 8mm. The width of the porous slit is b_{slit} = 1.2mm and the porosity ϕ = 0.36. But the measured penetration depth is more than 6 mm. This implies that the measured area is not filled completely anymore.

To explain why suddenly, with a different wettability the liquid penetration changes dramatically it is necessary to take a look at the work of Seeman et. al [18]. Their main result is shown in Fig. 8. They show that for an open channel for different aspect ratios and wettabilities, completely different wetting regimes occur. The corresponding droplet shapes can be seen on the right. Of course the case F-/cW is wetting a much larger area compared to case D. What is observed in the study at hand, has to be a similar effect. Also it can be seen that the filled area is not as transparent as in the other measurements. This also shows that there is no complete filling of the pores.

ACKNOWLEDGMENT

This work is supported by the Center for Smart Interfaces, TU Darmstadt. The help of the company Evonik is acknowledged. Special thanks go to Christian Schäfer and Alexander Nees.

NOMENCLATURE

Symbol	Quantity	SI Unit
a	ellipse axis 1	[mm]
b	ellipse axis 2	[mm]
b_{slit}	width of the slit	[mm]
D_{Pore}	pore diameter	[mm]
L	penetration depth	[mm]
r	initial drop radius	[mm]
$R1$	curvature radius 1	[mm]
$R2$	curvature radius 2	[mm]
t	time	[s]
V	Volume	[mm^3]
ϕ	porosity	[ ]
μ	dynamic viscosity	[mPa s]
π	pi	[rad]
Θ	contact angle	[°]
σ	surface tension	[mN/m]

REFERENCES

[1] K. Wallace, K. Yoshida, *Journal of Colloid and Interface Science*, vol. 63-1, p.164-165, 1978.

[2] S. Chandra, C.T. Avedisian, *Int. J. of Heat and Mass Transfer*, vol.35-10, p.2377- 2388, 1992.

[3] F.A.L. Dullien, Porous Media. Fluid Transport and Pore Structure, 2nd edition, Academic Press Inc., 1992.

[4] F. Oliver, *Tappi journal*, vol.67-10, p. 90-94, 1984.

[5] W. Cooper, L. Edwards, F. Hardaway, *U.S. Army Aberdeen Providing Ground Report* No.CRDEC-TR-112, 1983.

[6] N.C. Reis, R.F. Griffiths, M.D. Mantle, L.F. Gladden, *Int. J. of Heat and Mass Transfer*, vol.46-7, p.1279-1292, 2003.

[7] K. Hapgood, J. Litster, S.R. Biggs, T.Howes, *J. of Col. and Interface Science*, vol.253-2, p.353-366, 2002.

[8] T. D'Onofrio, H. Navaz, B. Markicevic, B.A. Mantooth, and K.B. Sumpter, *Langmuir*, 26-5, p.3317, 2010.

[9] A. Clarke, T. D. Blake, K. Carruthers, and A. Woodward, *Langmuir*, 18-8, p.2980–2984, 2002.

[10] N. Allenborn, H. Rasziller, *Chemical Engineering Science*, vol.59, p. 2071-2088, 2004.

[11] N. Reis, R. Griffiths, J. Santos, *Applied Mathematical Modelling*, vol.32, p.341-361, 2008.

[12] P. Alam, M. Toivakka, K. Backfolk, P. Sirviö, *Chemical Engineering Science*, 62, p.3142 – 3158, 2007.

[13] C. Batz-Sohn, A. Lembach, L. Nelli, A. Müller, I. Roisman, C. Tropea, *NIP26 26th International Conference on Digital Printing Technologies and Digital Fabrication*, Austin Texas USA, sept. 2010.

[14] Edward W. Washburn, *Physical Review*, 17-3, p.273, 1921.

[15] A. Gipperich, A. N. Lembach, I. V. Roisman and C. Tropea, *23rd International Conference on Liquid Atomization and Spray Systems*, Brno, Czech Republic, September 2010.

[16] P.S. Laplace, Mécanique céleste, Supplement to the tenth edition, 1806.

[17] A.N. Lembach, C. M. Weickgenannt, S. Goertz, I.V. Roisman and C. Tropea, *Atomsation and Sprays* (submitted 2011)

[18] R. Seemann, M. Brinkmann, E. J. Kramer, F. F. Lange, and R. Lipowsky, *Proc. Nat. Acad. Sci.*, vol.102, p.1848, 2005.

Table 1. Parameter variation

Pore sizes	small: 36µm		mid: 90 µm		big: 202 µm	
Fluids	distilled Water		Toluene- Diiodomethan			
Drop Size (water)	2.71mm		2.11mm		2.08mm	
Drop Size (toluene..)	2.01mm		1.65mm		1.55mm	
Release height	~0cm	1cm	5cm	20cm	50cm	1m
Wettability (water)	(0°) No drop		(165°) Tego Top 210		(20°) plain glass	

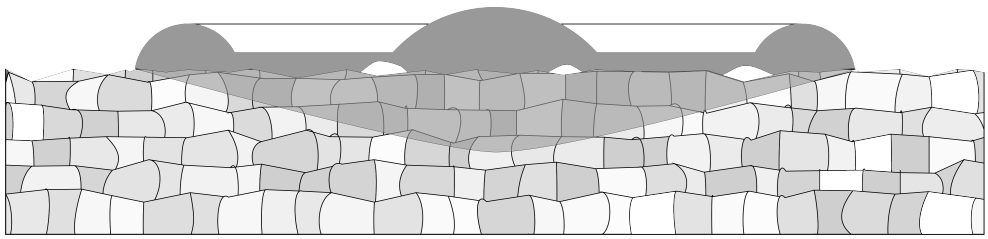

Figure 1. Sketch of drop impact on porous media

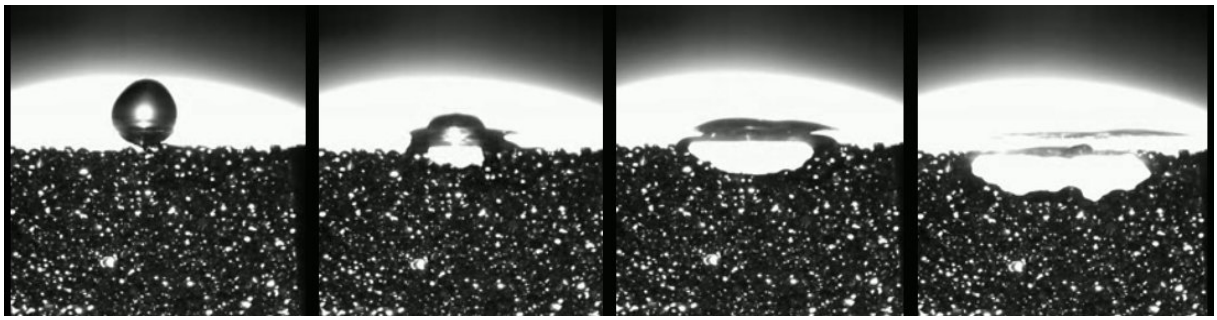

Figure 2. Typical result of a millimeter size drop impacting on a porous substrate (0.01sec total)

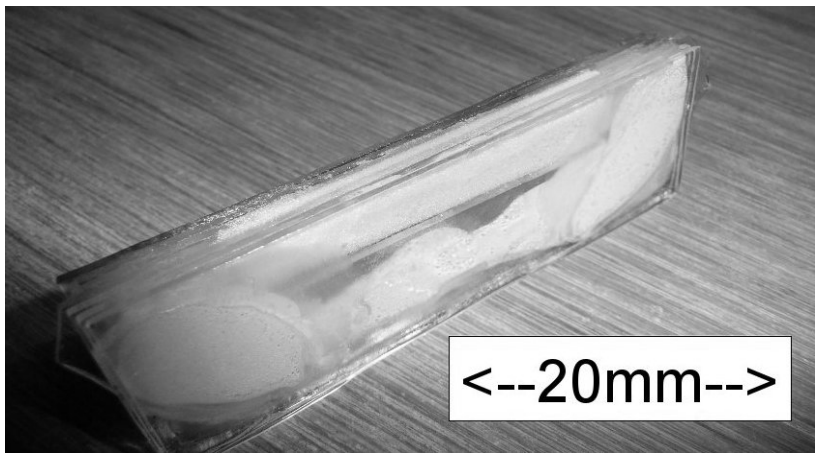

Figure 3. A porous target – glass beads sintered in slit

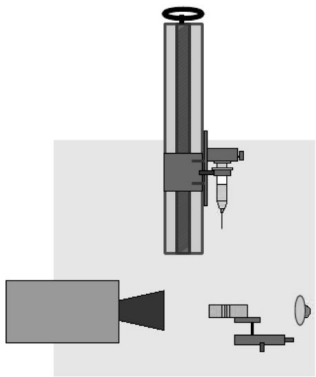

Figure 4. Experimental Setup

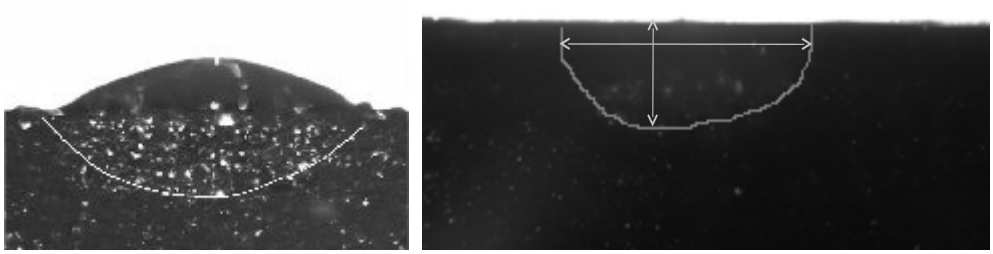

Figure 5. Two results of automatic detection of liquid front in porous medium for water

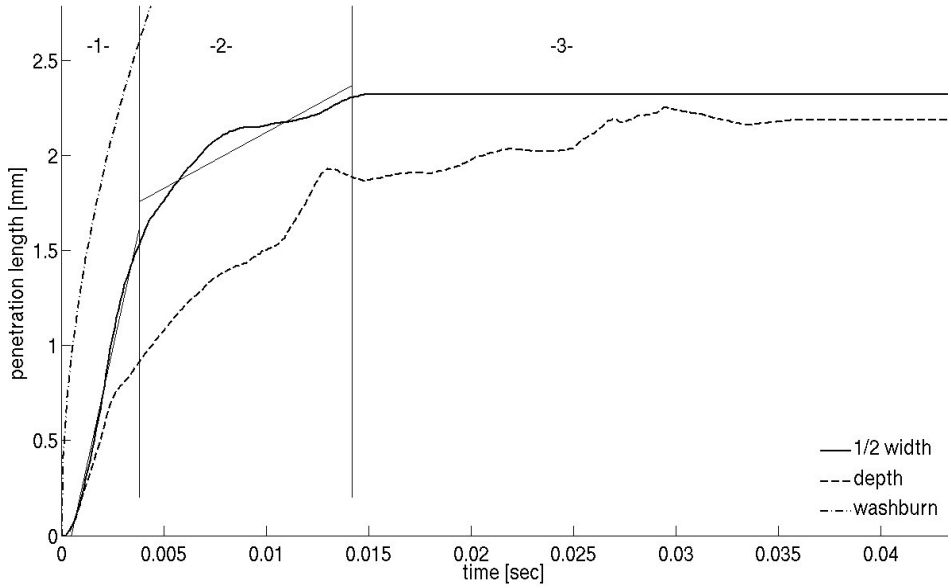

Figure 6. Penetration depth and ½ width over time compared with Washburn (Toluene-mix; 2.01mm drop diameter; 0.5m/s impact velocity; 202µm pore size)

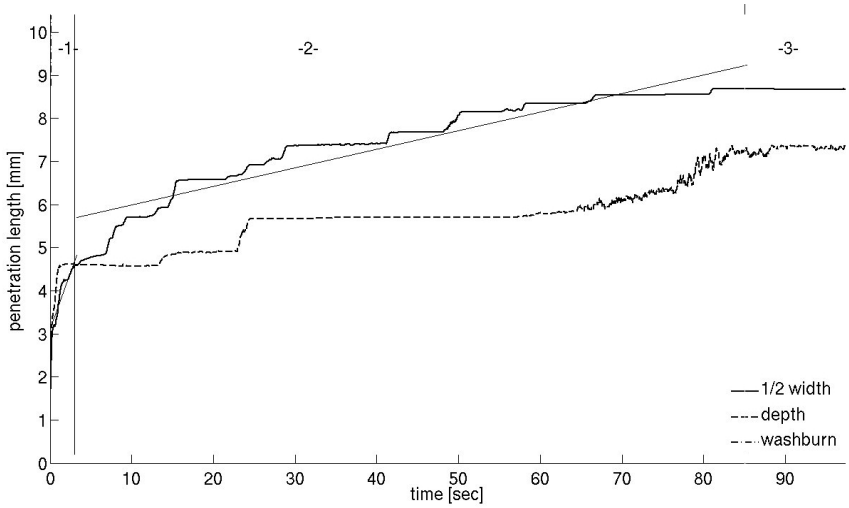

Figure 7. Penetration depth and ½ width over time compared with Washburn (Water; 2.08mm drop diameter; 0m/s impact velocity; 202µm pore size, 3° contact angle)

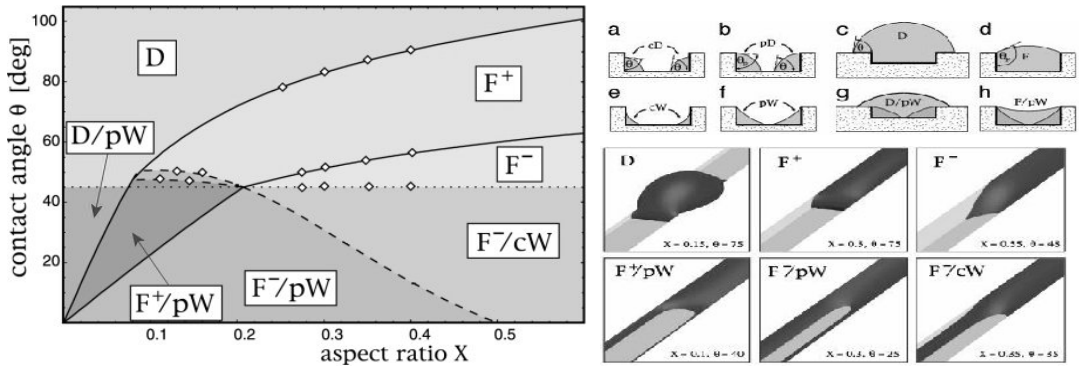

Figure 8. Wettability and channel aspect ratio affect the wetting regimes as shown on the right [18]